2013 International Conference on Virtual Reality and Visualization

An Interactive Warping Method for Multi-channel VR Projection Display Systems with Quadric Surface Screens

Fang Sun
School of Computer and Information Technology,
LiaoNing Normal University
Dalian, China
sf8552@126.com

Weiliang Meng
LIAMA - NLPR, CAS Institute of Automation

Beijing, China
weiliang.meng@ia.ac.cn

***Abstract*—In this paper, we present a practical non-camera-based interactive warping method for multi-channel immersive VR projection display systems with quadric surface screens. Instead of using one or multiple cameras as most previous methods did, we employ a commercial theodolite and a mouse to interactively calibrate each projector on site. By taking advantage of the nature of shape of the curved screen, we are able to perform fast, robust projector calibration and compute the warping map for each projector by taking other system information into account, i.e., position/frustum of the designed eye point (DEP). Compared with camera-based solutions, our method is accurate, cost-effective, simple to operate, and can reduce system set-up time and complexity efficiently. The feasibility of our method has been verified by many real site installations.**

Keywords- VR, Warping, Calibration, Multi-channel Projection System

I. INTRODUCTION

A. VR Projection Display System

Virtual Reality System, also known as VR System, has been developed over decades and applied in various professional fields ranging from mission-critical training to scientific visualization [1]. To achieve visual immersion, a VR system normally contains a multi-channel seamless projection display system that displays virtual 3D scene with a big field of view (FOV) on a curved screen, the shape of which is usually a part of a quadric surface, i.e., either spherical/cylindrical as usual, or conical, ellipsoidal or even paraboloidal for special applications [2]. Planar screens can also be an alternative for VR systems in terms of CADWalls and CAVEs [3]. Differing from 2D large-scale display systems which show “wallpaper” like content, VR systems introduce the concept of Designed Eye-point (DEP) and DEP-based viewing frustum for each projection channel, making each projection image a view of the 3D virtual scene from the DEP. Generally, a VR projection display system consists of the following components:

- A screen, typically curved with regular quadric shape, i.e., a dome or a cylinder.
- Multiple projectors, with either internal or external warping and edge-blending hardware/software module.
- A designed eye-point (DEP) which theoretically is the only spot having the correct geometrical view of the virtual 3D scene in the site. In case of VR stereo display, there are two DEPs (left and right). In such cases, the projection image group for the left eye will be warped according to the position of the left DEP, and the same for the right eye.
- DEP-based viewing frustums, each of which corresponding to a projection image.

Figure 1 shows the components of a typical VR display system.

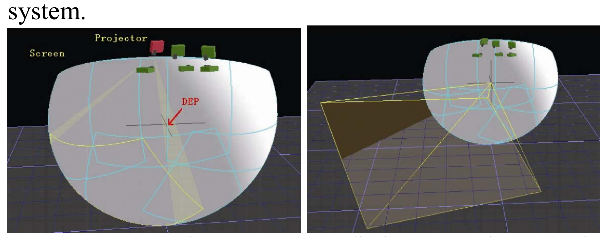

Figure 1. Typical structure of a VR display system: the screen, the projectors, the DEP and a DEP-based viewing frustum (the yellow pyramids in the right figure) corresponding to a projection image (the domain surrounded by the yellow lines on the screen in the left figure)
.

In addition to the above components, a VR system also contains an Image Generator (IG) at the back, which renders the 3D virtual scene for each projector in real-time according to the corresponding DEP-based viewing frustum.

In VR multi-channel seamless projection systems, there are 3 key independent technical issues, i.e., projection image warping, edge-blending and colour balancing. This paper focuses on projection image.

B. Background

Camera-based Warping Solution

Image warping for multi-channel, large scale projection systems, also known as geometry registration or image alignment, is a well-studied research topic in computer vision and computer graphics [4]. Most literature in this field focused on aligning projection images based on one or multiple cameras. For planar screens, this problem has been addressed as calculation of homography matrices between the camera and projectors [5]. To achieve this, either some of the parameters of the camera/projectors have to be previously known, or physical fiducials have to be used in the site for the calibration purpose. Takayuki et al. [6] proved that with a single uncalibrated camera and projectors

978-0-7695-5150-0/13 $26.00 © 2013 IEEE
DOI 10.1109/ICVRV.2013.9

whose entire intrinsic parameters but focal length are known, the minimum number of projectors needed for automatic warping on a planar screen with a single test image is 4. They also stated that by using a partially calibrated camera in which only focal length is unknown, the minimum number of projectors can be reduced from 4 to 3. Garcia-Dorado et al. [7] removed the need of knowing projector intrinsic parameters but added visible fiducials at corners of the projection image. Previous works on planar screen image registration are important for quick setup of systems with a large number of projectors that are casually placed, i.e., systems in offices, labs or homes. However, for planar VR systems, to achieve best image quality and pixel usage, projectors are always very carefully set up with professional mounting kits. Meanwhile, the number of projectors is normally limited from 3 (CASWalls) to 5 (CAVEs). Tests and engineering practice show that in such an installation, with professional warping hardware, satisfactory image alignment can be manually achieved in a few minutes, similar to the time used by camera-based solutions. Therefore, this paper focuses on a more complex and widely-used scenario, image warping on curved screens.

Registering images from multiple projectors on curved screens requires 3D reconstruction of the screen surface, which in turn needs multiple cameras [8, 9, 10]. Most multi-camera-based curved screen image warping algorithms are complex and time-consuming. However, for static warping with a stationary DEP, avoiding 3D screen surface reconstruction is possible due to the fact that warping in such cases is actually a stable 2D mapping from the DEP-based image space to the projection image space (see section II). Raskar et al. [11] proposed a way to perform warping and edge-blending on arbitrary shape screens with uncalibrated projectors and an uncalibrated camera. They used a wide-field-of-view camera locating at the DEP that can see the entire projection area. With this camera, it is possible to establish per-pixel mapping relationship between the camera image space and the projection image space. Bi-linear interpolation is used to handle pixel occlusion and noise. For VR systems in this case, DEP-based viewing frustum for each projector couldbe denoted by its projection area in the camera. image. The best result may be obtained when the DEP-based viewing frustum is identical with the camera's. But this method is not suitable for systems that require high resolution, high accuracy and very large field of view. Due to the resolution difference between the camera and projectors, in practice it's difficult to establish the mapping in a per-pixel basis unless using a very expensive camera. As the camera is uncalibrated, although being able to see a seamless image, the viewer may be affected by incorrect angular view of the virtual scene. Brown et al. [12] considered these problems and employed projected fiducials (circles) instead of individual pixel to build the mapping relationship. They improved the observation accuracy by utilizing a calibrating camera, enabling them to perform precise warping with an inexpensive commercial camera for a single view point.

When the viewpoint is moving, dynamic warping is indispensable and the reconstruction of the screen is inevitable. In a VR system, the curved screen used normally are made into a regular shape, i.e., a quadric surface, or a part of it . This characteristic exerts constrains on image registration and therefore offers a possibility to simplify the warping process. Raskar et al. [13] introduced a simplified parametrized transfer equation for warping on quadric surfaces. Sajadi and Majumder [14] proposed an efficient automatic method to calibrate projectors on fiducial-free piecewise smooth vertically extruded surfaces using a single un-calibrated camera. By introducing a dimension reduction technique, they were able to calibrate the camera and in turn all projectors by taking advantage of the four corner points and top/bottom edge of the screen. Once the camera is calibrated, screen geometry can be estimated and therefore the viewpoint (DEP) can be anywhere in the site. Impressive results were obtained on both cylindrical screens and CAVEs. However, assumptions are also needed for this method, i.e., the aspect ratio of the rectangle formed by the four corners of the surface should be known and the boundary is supposed being visible and segmentable. Meanwhile camera intrinsic parameters need to be known as well, although not from the calibration.

Most camera-based novel researches on image auto-warping assume that the camera can see the entire projection image area in one time. This is not possible in practice when it comes to VR systems with large curved screens or big FOV. To be practical, a pan-tilt unit (PTU) may be utilized, which allows the camera to have multiple views of the projection area. The use of PTU can greatly improve the practicality and scalability of a warping solution. Sajadi et al. [15] introduced a PTU-based multi-view warping method using an uncalibrated camera for vertically extruded surface screens. Spectacular accuracy and scalability was achieved by applying this algorithm which assumes the camera center of projection (COP) is coincident with the center of rotation of the PTU. As reported, even with 200 camera views of the projection images, the algorithm can still get accurate results. They further improved PTU usability by allowing a translation between the center of rotation of the PTU and COP of the camera in [16], where they proposed their projector auto-calibration method on a dome with one single uncalibrated camera and one fiducial. Together with [14], novel methods they proposed were the first efforts toward fast image warping on regular shape curved screens with one uncalibrated camera.

Despite the nice feature of being fully automatic, camera-based warping solutions, have a few drawbacks. When the projection image area is bigger than the camera field of view, which very often occurs in VR display installation, the camera needs to be re-setup in order to accomplish full view of the site (the use of PTU, for example), making the process interactive and time-consuming. When part of the image hits outside of the screen, calibration result may not be accurate. Inaccuracy may also be introduced when the projection image resolution is higher than the camera CCD resolution. If there are obstacles between the camera and the projection image, i.e., a cockpit etc., warping will be severely affected. Setting up and integrating the camera into the system is rarely an easy job. Most camera-based solution needs a dedicate PC to control the camera and the projector simultaneously, both of which, make the solution complex and less cost-effective. Generally, on curved screens, camera-based solution is considerably time-saving only compared with the manual warping. For instance, warping on a three-channel dome system may take a few minutes to few hours for a camera-based solution while take a few days for manual alignment.

Non-Camera-based Warping Solution

Considering the drawbacks of camera-based solutions, attempts have been made to remove the camera from the loop in both novel and practical engineering arenas. Light sensors are employed in non-camera-based warping solutions to allow projectors to allocate their projection images on the screen surface automatically. Lee et al.[17] proposed a method that embeds light sensors at important feature locations of the display target and uses structured light patterns to discover each sensors location in projection image space. Their algorithm is fast and robust not only on planar screens but also on special shape display targets, given sensors are planted properly. 3D Perception [18] first introduced light-sensor-based technology into VR industry by promoting their smart screen product, the Northstar AuroraTM. In this product, light sensors are embedded into dome panels to give response to different test pattern images generated by the company's warping hardware and the projector, resulting in fast automatic projector calibration. When projector location varies, re-calibration takes only about 10 seconds per projector. On the other hand, although being very fast on calibration, light-sensor-based warping solutions are not efficient due to the time needed for setting up the screen. For example, building up an Aurora screen normally takes 1-2 days. At the same time, projector calibration may be affected by various factors such as screen panel installation errors, projector delays as well as environmental lighting conditions.

C. *Contribution of Our Work*

In this paper, we present a non-camera-based warping method for VR display systems. Our method has the following differentiators with previous solutions:

- Neither cameras nor sensors are needed. We only use COTS hardware, i.e., a theodolite and a mouse to calibration projectors.
- Projector intrinsic and extrinsic parameters don't need to be known in advance at all.
- No limitations on the number of projectors and projection layout.

Like previous methods, our method needs a few assumptions as well, which are reasonable and easy to be satisfied:

- Projectors are considered as dual of a pin-hole camera as assumed in [14].
- The screen is either front or rear projected. Collimated projection systems are not considered in this method.
- The screen is a part of a quadric surface whose parameters are known.

Our method consists of two parts: projector calibration and mapping definition. The projector calibration is an interactive process regardless of the shape of the screen. The mapping definition constructs the mapping relationship between the DEP-based image (the IG produced image) and the projection image by utilizing the screen grid generated by the quadric equation of the screen surface. Our method has similar efficiency with camera-based solutions but uses standard tools and very simple interactions. Devices used in our method are all COTS hardware which is inexpensive and easy to obtain. With only few mouse-clicks (typically 16 clicks per channel), we can calibrate the projector and then perform a very accurate warping in few minutes. As we use the display target, i.e., the screen itself as the reference object for the projector calibration, the calibrated projector model fits the display site exactly. In most cases, neither occlusions in projection light path nor missing of part of the projection image can corrupt the calibration. Together with the fact that no dedicate PC is needed, our method is efficient, convenient and cost effective. The accuracy, simplicity and efficiency of our method have been proven by many real site installations.

This paper is organized as follows: In section II, the principle of image warping in VR projection display system is briefly described, followed by the illustration of interactive projector calibration algorithm, as well as the implementation and error correction. In section III, the real on-site test results are shown to validate our interactive warping method. Finally, we conclude with future works in section IV.

II. Interactive Warping Method

A. *Image Warping in VR Display*

The essence of the image warping in VR projection display system is to resolve pixel directional deviation between the IG produced image and the reality. Since DEP is the only viewpoint for all projection channels, each pixel in each IGproduced image represents a viewing direction from the DEP with two degrees of freedom, i.e., the azimuth angle and the pitching angle. Theoretically, if the projector located at the DEP and the projector intrinsic/extrinsic parameters are identical with the IG frustum, i.e., the DEP-based frustum, there would be no need to warp the image. However, for actual curved screens, each pixel in an IG produced image is not projected to the correct location on the screen due to the unavoidable viewpoint/frustum difference between the projector and the IG. Image warping targets at "moving" every pixel in the IG-produced image back to its correct location in the projection image so that it appears at the right azimuth/pitch angle on the screen when being observed from the DEP. As processing all pixels takes too many computation resources, to be efficient and practical, interpolation is always used in image warping, i.e., only a few control points in the IG-produced image are warped and pixels inside are processed using non-linear interpolation. For this reason, screen grid is often used as the test pattern, making it easier to match a control point in an IG produced image to its target position on the screen. In the "old times" of visual simulation when warping was done manually, on-screen target positions of typical control points are marked as references by UV-sensitive materials that are visible in UV light but invisible in normal light, making alignment possible without interfering normal use of the system. Later this approach was replaced by laser arrays [19] before modern warping solutions came forth.

To generate the test pattern, the screen is modeled and reticulated as grids, the density of which depends on the required warping accuracy. The vertices of the screen grid are used as control points. This screen grid is then put into the virtual database at the same location as it is in the real world, so that the IG can "look at" it from the DEP using the viewing frustum defined for each projector. For a projection channel, we use I_1 to represent the IG produced image and I_2 to represent the image in which all control points are at correct positions on the screen when being projected by the projector. Taking the lower-left channel in Figure 1 as an example, I_1 and I_2 with control points are shown in Figure 2. Then the warping is the control point mapping from I_1 to I_2.

Obviously, obtaining I_2 is the key of image warping. In the camera-based solution with a calibrated camera in a site where the screen shape is known, I_2 can be computed according to the relationship between the camera and the screen, given the camera can see the entire projection image [4]. However, noting the fact that a projector can be treated as a virtual camera [20] and the screen shape is regular, we can calculate I_2 in a simpler way. As all control points are on the virtual screen, taking a snapshot for the screen with the virtual camera (the projector) in the virtual scene will get I_2. To define and position this virtual camera correctly, we need to calibrate the projector.

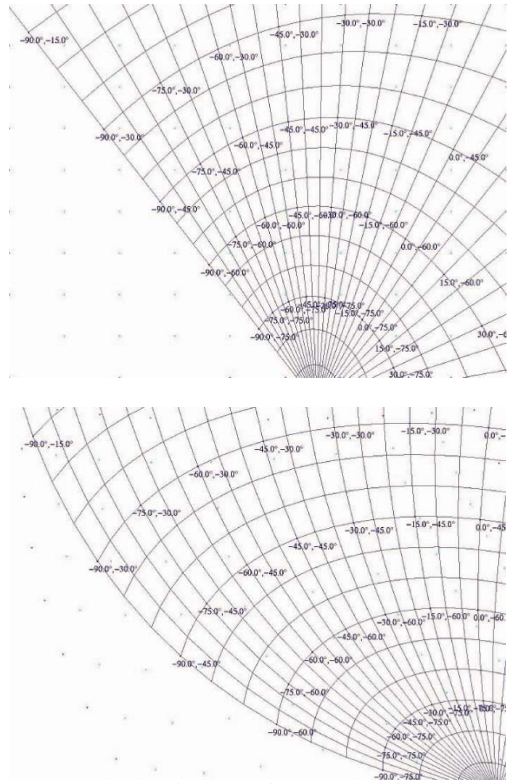

Figure 2. Image I_1 (top) and Image I_2 (bottom) of the lower-left channel in Figure 1.

B. *Projector Calibration*

We use the idea that Raskar et al. used on camera calibration in [8] to calibrate a projector. The differences in our method are a) we use the screen as the 3D reference object instead of markers and b) we decompose the projection matrix to get the projector intrinsic and extrinsic parameters so that the projector can be defined as a virtual camera with OpenGL commands. The DLT method allows us to calculate the projector intrinsic and extrinsic parameters at the same time, which is described in details as follows.

Let $O_u - uv$ be the image coordinate system on pixel basis and $O - xy$ being a related coordinate system based on pixel physical size, where O is the intersection point of the image plane and the projector optical axis, called the principal point. We have

$$\begin{pmatrix} u \\ v \\ 1 \end{pmatrix} = \begin{pmatrix} 1/dx & \gamma' & u_0 \\ 0 & 1/dy & v_0 \\ 0 & 0 & 1 \end{pmatrix} \quad (1)$$

where dx and dy are the physical lengths of a pixel along each axis respectively and γ' is the skew factor. We further establish the projector coordinate system $O_C - X_C Y_C Z_C$ where O_C is the optical center of the projector, Y_C is the projector up vector and Z_C is the optical axis. We have

$$\begin{pmatrix} X_C \\ Y_C \\ Z_C \\ 1 \end{pmatrix} = \begin{pmatrix} \mathbf{R} & \mathbf{t} \\ \theta^T & 1 \end{pmatrix} \begin{pmatrix} X_W \\ Y_W \\ Z_W \\ 1 \end{pmatrix} \quad (2)$$

where **R** and **t** are rotation matrix and translation vector respectively and $\theta^T = (0,0,0)^T$, $O_W - X_W Y_W Z_W$ is the world coordinate system. We define the distance between O_C and O as the focal length f , $f = |O_C O|$. The relationship between $O - xy$, $O_C - X_C Y_C Z_C$ and $O_W - X_W Y_W Z_W$ is shown in Figure 3.

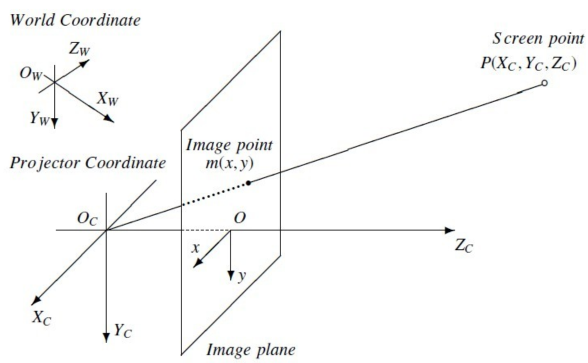

Figure 3. Coordinate systems and relationship between a point m on the image plane and its corresponding projection surface point P in the real world.

With the pinhole model, a point $m(x, y)$ on the image plane is projected onto a surface point $P(X_C, Y_C, Z_C)$, and the relationship between m and P can be written as

$$Z_c \begin{pmatrix} x \\ y \\ 1 \end{pmatrix} = \begin{pmatrix} f & 0 & 0 & 0 \\ 0 & f & 0 & 0 \\ 0 & 0 & 1 & 0 \end{pmatrix} \begin{pmatrix} X_C \\ Y_C \\ Z_C \\ 1 \end{pmatrix} \quad (3)$$

Together with (1) and (2), we have

$$Z_c \begin{pmatrix} u \\ v \\ 1 \end{pmatrix} = \begin{pmatrix} 1/dx & \gamma' & u_0 \\ 0 & 1/dy & v_0 \\ 0 & 0 & 1 \end{pmatrix} \begin{pmatrix} f & 0 & 0 & 0 \\ 0 & f & 0 & 0 \\ 0 & 0 & 1 & 0 \end{pmatrix} \begin{pmatrix} R & t \\ 0^T & 1 \end{pmatrix} \begin{pmatrix} X_W \\ Y_W \\ Z_W \\ 1 \end{pmatrix} \quad (4)$$

Equation (4) can be re-written as

$$Z_C \mathbf{m} = \mathbf{KEX} = \mathbf{PX} \quad (5)$$

where **K** and **E** are the intrinsic and extrinsic parameter matrix, respectively. P is the projection matrix, mis a group of pixels in image coordinate and X is the corresponding 3D surface points set in world coordinate.

Equation (5) indicates that if we know no less than six image points and their corresponding non-co-planar projection points on the screen surface, we will be able to solve P using a least-squares method[21]. By QR decomposition, we can compute K and E, which include:

Intrinsic parameters:

- Principle point $O(u_0, v_0)$, in $O_u - uv$ coordinate.
- Focal length f .

Extrinsic parameters in world coordinate:

- Optical center of the projector O_C .
- Projection axis vector $\vec{\mathbf{v}}$.
- Projector up-vector $\vec{\mathbf{u}}$.

C. Interactive Calibration Process

In practice, we use a theodolite putting at the center of the quadric screen to generate screen surface points. We install a small program on the IG node which roughly divides the projection image into 4×4 area and displays a cross at the pixel where the mouse clicks. When calibrate a projector, we first run the program and then perform the following steps:

- Step 1: Point the theodolite to a screen point roughly at the center of one of the 4×4 area, record its azimuth and pitch angle as well as its distance to the center of the theodolite. The theodolite will produce a laser dot on the screen.
- Step 2: Use the mouse to click on the laser dot. This will produce a cross on the screen. Then use arrow keys to finely tune the position of the cross until the center of which best overlaps with the laser dot. The program will record this pixel coordinate.
- Step 3: Repeat Step 1 until all areas are done.

The distance measurement function of the theodolite makes it possible to calculate **X** according to the azimuth/pitch angle of each point selected on the screen, and the mouse clicks record **m** in terms of pixel coordinates in the image space. The curvature of the screen guarantees points being clicked throughout the projection image do not fall onto the same plane. When calibrating a projector, different reference objects will result in different parameters. In our method, we use the display target, i.e., the screen itself as the reference object, resulting in the best fit of the projector model to the particular site.

After getting **X** and **m** from above steps, both intrinsic and extrinsic parameters are calculated by optimizing Equation (5). We use these parameters to define the virtual camera in the virtual scene. Taking a snap shot for the screen grid and control points with this camera will produce I_2 .

D. Error Correction

Various reasons can introduce errors into the calibration data, i.e., imperfection of the screen shape, inaccurate placement of the theodolite and projector lens distortion, etc.

Sometimes a pixel can never cover the center of the laser dot due to the fact that projectors are discrete devices while a theodolite is not. Unpredictable as these errors are, as what we find in practice, they can be well corrected or compromised between adjacent projection images by employing a simple manual warping mesh on top of image I_2, which can be a 5×5 mesh with linear interpolation(See Section III).

III. Real On-site Test Results

We performed the real site test on two projection channels (lower-left and lower-middle channel) in Figure 1 using our interactive warping algorithm. The projectors used are Christie DS+10K-M with 1.2:1 fixed lens and 1400x1050 resolution. The warping device we use is Christie build-in warping unit Twist^{TM}. The mapping of the 10x10 control point mesh is written into Twist^{TM} control data file in terms of a four-column table whose first two columns are control point image coordinates in I_2 and third and four column are their regular image coordinates in I_1, part of which is shown below (lower-left channel):

```
< mesh rows='10' cols='10' width='1400' height='1050'>
<point x='38.000000' y='-8.000000' orgX='0.000000' orgY='0.000000'/>
<hTangent type='auto'/>
<vTangent type='auto'/>
<point x='134.000000' y='8.000000' orgX='155.555556' orgY='0.000000'/>
. . . . . .
```

The radius of the dome is 2.9 meters. Figure 4 shows the marking points of the two channels on the screen. Note part of lower-left hits outside the screen. The total marking time for these two channels including setting up the theodolite is 10 minutes and the calculation time is less than 1 second. Manual fine tuning for the two channels takes 5 minutes. Table 1 shows the marking points of lower-left channel in both image coordinate and world coordinate. Calibration results of the two channels are shown in Table 2 and 3. Figure 5 shows the un-warped test pattern and Figure 6 shows the same pattern after warping based on above calibration Results. Figure 7 shows the un-warped display of a virtual 3D database. Figure 8 shows the same scene after warping and edge-blending.

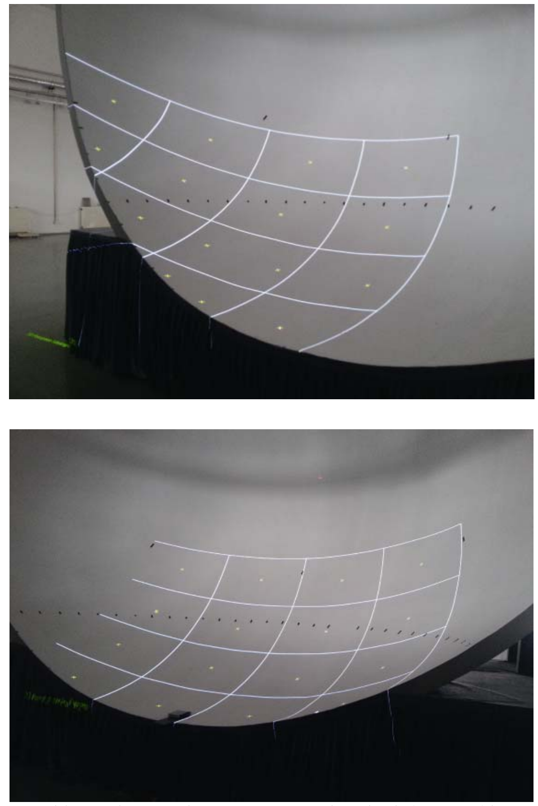

Figure 4. Marking points on the screen. Note that the left part of lower-left channel has hit outside the screen.

Table 1: Marking points of lower-left channels.

Mouse Click	Image points m		Screen points X		
	u	v	X_w	Y_w	Z_w
1	170	139	-2.599	-1.116	-0.753
2	517	132	-1.959	-1.42	-1.684
3	885	143	-0.964	-1.603	-2.262
4	1219	142	-0.034	-1.597	-2.448
5	211	399	-2.424	-1.591	-0.425
6	515	396	-1.847	-1.946	-1.173
7	876	407	-0.89	-2.181	-1.73
8	1206	416	0.017	-2.188	-1.899
9	361	660	-2.02	-2.103	-0.198
10	644	650	-1.418	-2.418	-0.772
11	904	662	-0.742	-2.581	-1.08
12	1209	682	0.051	-2.604	-1.212
13	647	847	-1.329	-2.568	-0.218
14	835	900	-0.869	-2.737	-0.312
15	1035	922	-0.386	-2.807	-0.42
16	1267	962	0.137	-2.806	-0.42

Table 2. Calibration result: projector optical center and optical axis.

Projector No.	Center of Projector OC	Optical axis $\vec{v}$
1	(-1.19818,0.43219,2.74404)	[-1.04238,-2.89005,-3.74404]
2	(-0.168035,0.544328,2.86729)	[-0.0293259,-2.77329,-3.86729]

Table 3. Calibration result: up-vector, principal point and focal length.

Projector No.	Up-vector $\vec{u}$	Principle point $O(u_0, v_0)$	focal length f
1	[1.80209 -10.673 7.73686]	(360.202,568)	1718.61
2	[0.65347 -10.5554 7.56447]	(623.007,599.281)	1791.45

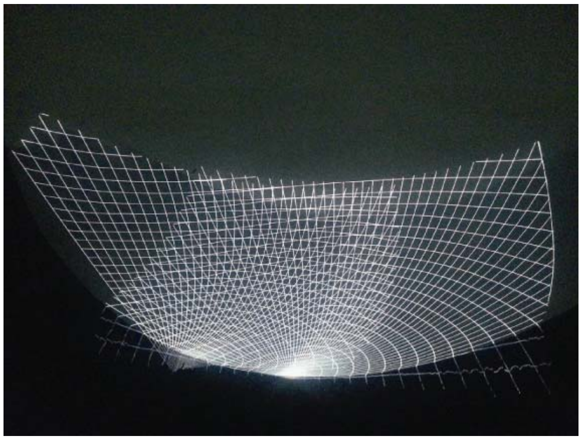

Figure 5. Unwarped test pattern.

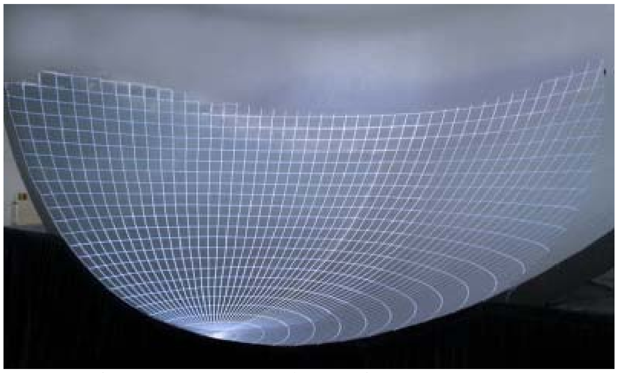

Figure 6. Test pattern after warping.

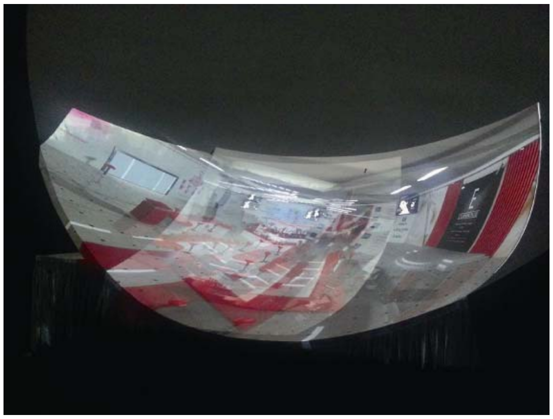

Figure 7. Un-warped display of the virtual scene.

Figure 8. Display of Virtual scene after warping and edge-blending.

The real site test shows that the calibration result is accurate enough even part of the projection image is missing on the screen. The manual tuning is subtle as shown in Figure 9, in which a 5×5 linear manual mesh is applied for the lower-left channel.

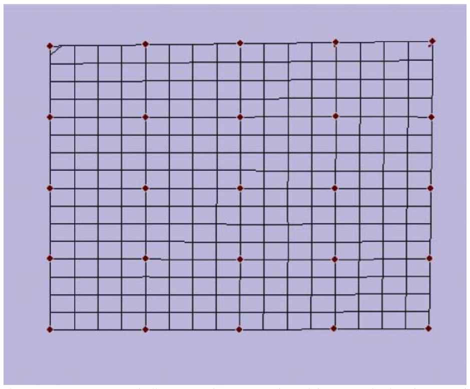

Figure 9. Manual fine tuning mesh of lower-left channel.

IV. CONCLUSION AND FUTURE WORKS

In this paper, we propose an interactive warping method for VR multi-channel projection display systems with quadric surface screens. Our target is designing a very practical solution for simple, fast and inexpensive system setup. Unlike previous warping solutions where one or multiple cameras are used, our method calibrates each projector with only a few interactions and offers similar efficiency in a simpler and more flexible manner. Both real site and experimental results validate our method being an accurate, robust, scalable and practical solution, which significantly saves the installation time and the cost for VR industry.

Our future works include developing this method to dynamic warping that supports moving DEP, as well as integrating the warping algorithm into commercial IG runtime applications such as VegaPrimeTM [22]. We are also developing a motor-driven theodolite that can measure not only the distance but also the light intensity, which will provide us a fully-automatic manner to scan the screen and accomplish the warping with higher accuracy on arbitrary curved screens.

ACKNOWLEDGMENT

This project is supported by the 2013 Annual Beijing Technological and Cultural Fusion for Demonstrated Base Construction and Industrial Nurture (No. Z131100000113007), and the National Natural Science Foundation of China (Nos. 61202324, 61271431, and 61271430).

REFERENCES

[1] Balci O, Bertelrud AI, Esterbrook CM, Nance RE. Introduction to the visual simulation environment. In: Proceedings of the 1997 Winter Simulation Conference. CA; 1997, p. 698–705.

[2] Brey P. The ethics of representation and action in virtual reality. Ethics and Information Technology 1999;1:5–14.

[3] Cruz-Neira C, Sandin DJ, Defanti TA. Surround-screen projection-based virtual reality: The design and implementation of the cave. In: Proceedings of the 20th Annual Conference on Computer Graphics and Interactive Techniques. ACM SIGGRAPH; 1993, p. 135–42.

[4] Brown M, Majumder A, Yang R. Camera-based calibration techniques for seamless multi-projector displays. IEEE Transactions on Visualization and Computer Graphics 2005;11:193–206.

[5] Sukthankar R, Stockton RG, Mullin MD. Smarter presentations: Exploiting homography in camera-projector systems. In: Proceedings of the Eighth International Conference On Computer Vision (ICCV-01). IEEE Computer Society; 2001, p. 247–53.

[6] Okatani T, Deguchi K. Easy calibration of a multi-projector display system. International Journal of Computer Vision 2009;85:1–18.

[7] Garcia-Dorado I, Cooperstock J. Fully automatic multi-projector calibration with an uncalibrated camera. In: Computer Vision and Pattern Recognition Workshops (CVPRW). 2011 IEEE Computer Society Conference on; 2011, p. 29–36.

[8] Raskar R, Brown MS, Yang R, Chen WC, Welch G, Towles H, et al. Multi-projector displays using camera-based registration. In: Proceedings of IEEE Visualization 99. San Francisco, CA; 1999, p. 161–9.

[9] Johnson T, Welch G, Fuchs H, Laforce E, Towle H. A distributed cooperative framework for continuous multi-projector pose estimation. In: proceedings of IEEE Virtual Reality. Lafayette, LA; 2009, p. 35–42.

[10] Cotting D, Fuchs H, Ziegler R, Gross MH. Adaptive instant displays: Continuously calibrated projections using per-pixel light control. In: Proceedings of Eurographics 2005. Eurographics Association; 2005, p. 705–14.

[11] Raskar R, Welch G, Fuchs H. Seamless projection overlaps using image warping and intensity blending. In: Proceedings of Fourth International Conference on Virtual Systems and Multimedia. Gifu: IOS Press; 1998, p. 179–88.

[12] Brown MS, Seales WB. A practical and flexible tiled display system. In: Proceedings of the 10th Pacific Conference on Computer Graphics and Applications. IEEE Conference Publications; 2002, p. 194–203.

[13] Raskar R, Baar J, Baar J, Beardsley P, Beardsley P,Willwacher T, et al. ilamps: Geometrically aware and self-configuring projectors. ACM Transactions on Graphics 2003;22:809–18.

[14] Sajadi B, Majumder A. Auto-calibrating projectors for tiled displays on piecewise smooth vertically extruded surfaces. IEEE Transactions on Visualization and Computer Graphics 2011;17:1209–23.

[15] Sajadi B, Majumder A. Scalable multi-view registration for multiprojector displays on vertically extruded surfaces. Computer Graphics Forum 2010;29:1063–72.

[16] Sajadi B, Majumder A. Automatic registration of multi-projector domes using a single uncalibrated camera. Computer Graphics Forum 2011;30:1161–70.

[17] Lee JC, Dietz PH, Maynes-Aminzade D, Raskar R, Hudson SE. Automatic projector calibration with embedded light sensors. In: Proceedings of the 17th Annual ACM Symposium on User Interface Software and Technology. ACM; 2004, p. 123–26.

[18] 3d perception: Smart screen. Online accessed 7-April-2013. URL http://www.3d-perception.com/sider/3d-perception-simulation.asp?NodeID=1051&PlaID=2.

[19] Barco: Barco's ldat (laser diode array tool). Online accessed 7-April-2013. URL http://www.barco.com/en/Products-Solutions/Visual-display-systems/3D-Display-management/Barcos-LDAT%e2%84%a2-Laser-Diode-Array-Tool-marks-reference-patterns-to-effectively-align-display-channels.aspx.

[20] Bimber O. Multi-projector techniques for real-time visualizations in everyday environments. In: IEEE VR 2006Workshop on Emerging Display Technologies. IEEE Computer Society Visualization and Graphics Technical Committee; 2006, p. 33–3.

[21] Faugeras O. Three-Dimensional Computer Vision: A Geometric Viewpoint. MIT Press; 1993.

[22] Presagis: Vega prime5.0. Online accessed 7-April-2013. URL http://www.presagis.com/products_services/products/modeling-simulation/visualization/vega_prime/.